The 2010 IEEE/RSJ International Conference on
Intelligent Robots and Systems
October 18-22, 2010, Taipei, Taiwan

A Magnetic Type Tactile Sensor by GMR elements and inductors

Masanori Goka, Hiroyuki Nakamoto and Satoru Takenawa

Abstract— **A novel magnetic type tactile sensor is proposed. This sensor can measure a three-axis force vector and detect a slip. The structure is simple, and this sensor consists of two layers, an elastic layer and a substrate layer. The elastic layer is made of an elastic material and has a cylindrical permanent magnet. The substrate layer is a glass epoxy board and has four GMR(giant magneto resistance) elements and four chip inductors. Each element outputs voltages as to a magnetic flux density when the elastic layer deforms by a contact. A force vector and a slip detection are calculated from these outputs. Laboratory experiments demonstrate the effectiveness of this tactile sensor.**

I. INTRODUCTION

In recent years, there have been a lot of researches of multi-fingered robot hands in order to realize an universal robot hand [1]-[3]. An universal robot hand can be applied to an industrial manipulator or a humanoid robot. It is important that a robot hand be equipped with tactile sensors that can detect slips and measure grasping force vectors for the implementation of complex and dexterous manipulations [4].

Some 6-axis force/torque sensors that built into finger tips have been used for measurements of grasping force vector and dexterous manipulations. These sensors have been downsized [5]. However, they are expensive and are not able to detect slips. There are various three-axis tactile sensor in some studies. Kobayashi et al. developed a prototype three-axis tactile sensor using a two-dimensional array of silicon structures with fixed strain gages [6]. It is difficult and expensive to manufacture a tactile sensor that has an array of strain gages. Ohka proposed a method by which to measure a force vector by utilizing the variation of refractive index in a fingertip-shaped optical waveguide [7]. Application of the optical-based tactile sensor to a robot finger is easy, but the sensor system requires an imaging device. Shinoda et al. proposed a tactile sensing element based on an ultrasonic cavity and verified the ability to detect the friction coefficient by measuring the resonant frequency of the cavity experimentally [8]. In their approach, the sensor enables the coefficient of friction to be detected at the moment of contact, but it is difficult to downsize the sensor element. Slips are detectable by a piezoelectric device. Son et al. developed a tactile sensor with strips of piezoelectric film to detect incipient slips and occurrences of contact [9]. However, it is difficult to measure a force vector by the sensor. Jockusch et al. prototyped a tactile sensor using a piezoresistive and a piezoelectric device, which are stacked in layers, to perform simultaneous measurement of contact force and position, and slippage detection [10]. This hybrid sensor make peripherals cumbersome and complicated.

We proposed a magnetic type tactile sensor. This tactile sensor can measure a three-axis force vector and detect a slip simultaneously. We have studied another magnetic type tactile sensor using a two-dimensional array of chip inductors [11]. Because an inductor can detect a magnetic flux density at a deformation, we calculated a three-axis force vector from inductors' output voltages. However, this tactile sensor had a large error of calculated force vector, and we have to improve it. In this paper, we proposed a magnetic type tactile sensor which consists of GMR elements and chip inductors. A three-axis force vector is calculated from GMR elements' output voltages, and a slip is detected from inductors' output voltages. Features of the tactile sensor are a wiring reduction, simple structure and low cost. In the following sections, the structure and principle of the proposed sensor is described. Formulas to transform output voltages of the proposed sensor into a force vector and a slip detection algorithm are described. Laboratory experiments demonstrate the effectiveness of the proposed sensor.

II. MAGNETIC TACTILE SENSOR

A. Structure and Principle

The proposed magnetic tactile sensor is composed mainly of two layers (Fig. 1), an elastic layer and a substrate layer. The elastic layer is made of an elastic material, for example, a silicon rubber or an urethane gel, and involves a cylindrical permanent magnet. The substrate layer is made of a glass epoxy board. The substrate layer's surface side is flat. There is no electronic part on the surface side. On the other hand, the substrate layer's back side has four GMR elements and four chip inductors. The elastic layer is fixed on the substrate layer's surface with an adhesive bond. Because these layers are not hard-wired, a breaking of wire do not happen. If an elastic layer is worn after a long-term usage, it is easy to replace an old elastic layer with a new one.

When the tactile sensor touches an object, the surface of elastic layer is displaced. The magnet in the elastic layer is also displaced depending on the elastic layer's deformation. This magnet displacement changes the magnetic flux density to the substrate layer's GMR elements, and outputs of GMR are changed. In a basic experiment, we changed distances between a magnet and a GMR element (Fig. 2). The magnet was moved within the range of $-5 \leq x \leq 5$, $-3 \leq z \leq 0$.

This work was not supported by any organization

M. Goka and H. Nakamoto are with Depertment of Infomation Technology, Hyogo Prefectural Institute of Technology, 3-1-12 Yukihira-cho, Suma-ku, Kobe, Japan {goka, nakamoto}@hyogo-kg.go.jp

S. Takenawa is with the Kobe City College of Technology, 651-2194, Kobe, Japan takenawa@kobe-kosen.ac.jp

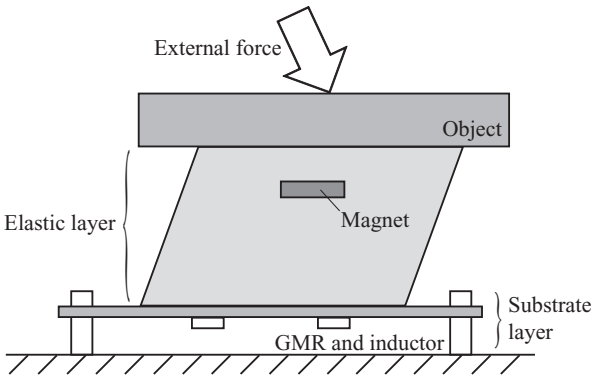

Fig. 1. Proposed sensor structure

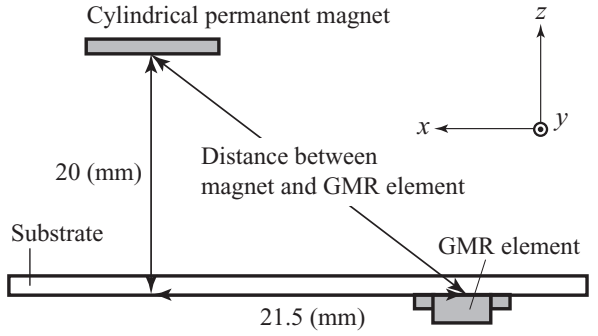

Fig. 2. Setup of a basic experiment

The relationship of GMR element's outputs and distances between a magnet and a GMR element is shown in Fig. 3. The GMR element was AA003-02 (NVE Corporation). The magnet was a cylindrical neodymium magnet which was $\phi 10$ mm in diameter, and its thickness is 1 mm. The magnetic flux density is 320 mT at the surface of the magnet. Because GMR's outputs were changed depending on distances between the magnet and the GMR element, it is possible to calculate a magnet's displacement vector and a displacement vector of the elastic layer's surface from outputs of three or more GMR elements. Moreover, a force vector is also calculated from those outputs of GMR elements with force vector's calibration values. GMR elements provide displacement and force vectors of elastic layer's surface as described above.

An inductor generates induced electromotive force depending on how much a magnetic flux density changes. An induced electromotive force is significantly generated by velocity of a magnetic flux density change rather than by amount of that. This means that the proposed tactile sensor's inductors generates higher outputs when the elastic layer's surface deforms rapidly. One of the examples of high-speed deformation on the elastic layer's surface is a stick-slip phenomenon which sticks and slips repeat alternately. An inductor can generate a large output at the moment of slip. Then, inductors provide slip detection of elastic layer's surface as described above.

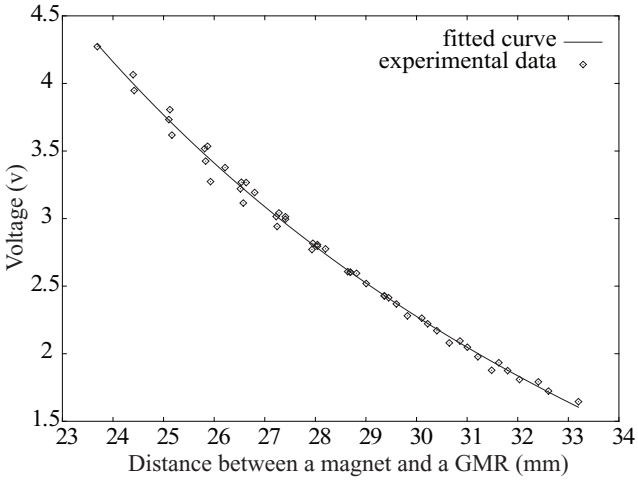

Fig. 3. GMR's output voltage vs. distance between GMR and magnet

B. Displacement and Force Vectors Calculation

Displacement and force vectors of the elastic layer's surface are calculated from four GMR elements' outputs. This calculation requires calibration values of GMR elements' outputs, displacement and force vectors of grid reference points $p_j (j = 1..J)$, which are distributed in the displacement range of the elastic layer's surface. J is number of reference points. The calculation procedure is shown as follows.

1) Four GMR elements' Outputs $V_{GMR_i} (i = 1..4)$ are measured.
2) Differences between measured GMR outputs and reference points' GMR outputs are calculated by

$$s_j = \sum_{i}^{4} |V_{GMR_i} - V_{GMR_i}^{p_j}| \quad (1)$$

where $V_{GMR_i}^{p_j}$ is GMR_i's output of reference point p_j.
3) Three reference points which s_j are smaller are defined as neighborhood points $\hat{p}_k (k = 1..3)$ of the measured GMR outputs.
4) GMR outputs' gradients with respect to displacement vector of neighborhood points $\hat{p}_k$ are expressed by $\frac{V_{GMR_i}^{\hat{p}_k}}{dx}$, $\frac{V_{GMR_i}^{\hat{p}_k}}{dy}$, $\frac{V_{GMR_i}^{\hat{p}_k}}{dz}$ of x, y, z-axis. Relative displacement vectors of neighborhood points $\hat{p}_k$ are expressed by $\Delta x^{\hat{p}_k}, \Delta y^{\hat{p}_k}, \Delta z^{\hat{p}_k}$. The following equation is formed.

$$\begin{aligned} V_{GMR_i} &= V_{GMR_i}^{\hat{p}_k} + \Delta x^{\hat{p}_k} \frac{V_{GMR_i}^{\hat{p}_k}}{dx} \\ &\quad + \Delta y^{\hat{p}_k} \frac{V_{GMR_i}^{\hat{p}_k}}{dy} + \Delta z^{\hat{p}_k} \frac{V_{GMR_i}^{\hat{p}_k}}{dz} \quad (2) \end{aligned}$$

5) We can solve (2) as four simultaneous equations of GMR's outputs. $\Delta x^{\hat{p}_k}, \Delta y^{\hat{p}_k}, \Delta z^{\hat{p}_k}$ are calculated by the pivot operation and Gaussian elimination, and displacement vector $\Delta x_k, \Delta y_k, \Delta z_k$ are also calculated from them and the displacement vector of $\hat{p}_k$.

6) 4) and 5) are repeated with two other neighborhood points $\hat{p}_k$, and the displacement vector of elastic layer's surface $\Delta\hat{x}, \Delta\hat{y}, \Delta\hat{z}$ are average values of $\Delta x_k, \Delta y_k, \Delta z_k$.

The Force vector acting on the elastic layer's surface is calculated from the displacement vector of elastic layer's surface $\Delta\hat{x}, \Delta\hat{y}, \Delta\hat{z}$. The reference point that is the nearest from this displacement vector in the Euclidean distance is selected, and the relative displacement vector of this selected reference point is expressed by $\Delta\tilde{x}, \Delta\tilde{y}, \Delta\tilde{z}$. Then, the following equation is formed using the force vector $F_x^{\tilde{p}}, F_y^{\tilde{p}}, F_z^{\tilde{p}}$ of the reference point and the force vectors' gradients with respect to displacement vector of the reference point.

$$F_x = F_x^{\tilde{p}} + \Delta\tilde{x}\frac{dF_x^{\tilde{p}}}{dx} + \Delta\tilde{y}\frac{dF_x^{\tilde{p}}}{dy} + \Delta\tilde{z}\frac{dF_x^{\tilde{p}}}{dz} \quad (3)$$

$$F_y = F_y^{\tilde{p}} + \Delta\tilde{x}\frac{dF_y^{\tilde{p}}}{dx} + \Delta\tilde{y}\frac{dF_y^{\tilde{p}}}{dy} + \Delta\tilde{z}\frac{dF_y^{\tilde{p}}}{dz} \quad (4)$$

$$F_z = F_z^{\tilde{p}} + \Delta\tilde{x}\frac{dF_z^{\tilde{p}}}{dx} + \Delta\tilde{y}\frac{dF_z^{\tilde{p}}}{dy} + \Delta\tilde{z}\frac{dF_z^{\tilde{p}}}{dz} \quad (5)$$

Because the right-hands of (3)-(5) are calculated from displacement vectors of the elastic layer's surface and calibration values of the reference point $\tilde{p}$, it is possible to calculate a force vector from the measured GMRs' outputs.

C. Slip Detection

The faster a magnetic flux density changes, the higher a induced electromotive force that an inductor generates is. In the moment of a stick-slip phenomenon, a deformed elastic layer becomes a normal shape rapidly, and a high induced electromotive force is generated. This high induced electromotive force at a stick-slip phenomenon is detected by three sigma limits. If the current output voltage V_{now} is in the following range, there is no possibility of a slip, and vice versa.

$$A - 3\sigma \leq V_{now} \leq A + 3\sigma$$

where N is number of time-series output voltages, σ standard deviation. Because the tactile sensor has four inductors, the slip is judged by all four possibility of slip.

III. EXPERIMENTS

A. Prototype

The layout drawing of GMR elements and inductors is shown in Fig. 4. The size of substrate is 100×100 mm and is 1 mm in thickness. Fig. 4 has xy-coordinates with their origin at the center of the substrate, and the unit of length is mm. The GMR elements and the inductors are placed at the positions of their coordinates. GMR3 and GMR4 are also on additional substrates of 1 mm and 2 mm in thickness. Then, they are not on the same xy-plane of GMR1 and GMR2. GMR elements are placed in the same orientation toward the substrate's center, because it becomes a cause of errors of output voltages by the differenct orientation. We use the

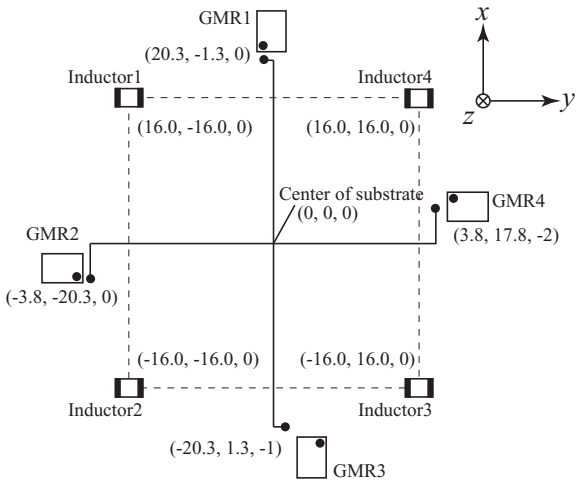

Fig. 4. Back side layout of substrate

GMR elements (AA003-02, NVE Co.) and the chip inductors (ELJFB102JF, Panasonic Co.) on this prototype.

Because of including a permanent magnet, there is a possibility that the elastic layer's pressure distribution becomes nonuniform on the surface. Then, we designed the elastic layer that its pressure distribution become uniform when a flat 10 N force acts on the surface by a finite element analysis. The size of cylindrical magnet model is $\phi 10$ mm in diameter, 1 mm in thickness, and we decided its initial position from Fig. 3. The elastic layer's material is a urethane gel (ASKER-C 15, Exseal Co.), and we set its physical property into the finite element analysis code (ADINA). The designed elastic layer is shown in section (Fig. 5). This elastic layer's surface is a gentle concave shape. If a flat 10 N force acts on the surface, this concave shape distributes a constant pressure. We manufactured the mold of the designed elastic layer, and the urethane gel became hardened in the mold in twice. The magnet was placed on the first hardened urethane gel, and the second urethane gel was poured into it. The prototype of tactile sensor is shown in Fig. 6. The upper white part is the elastic layer, and the substrate layer is under it. The substrate is 1 mm in thickness. To prevent a deflection when a force acts on the sensor, the substrate has eight spacers at the edges. Output voltages of GMRs are amplified fifteenfold by a differential amplifier, and those of inductors are amplified ten-thousandfold by two inverting amplifiers. Each output voltage is measured by a PC via a A/D converter board.

B. Experiments of Displacement and Force Vectors

Fig. 7 shows the experimental setup with the prototype tactile sensor. A vertical and horizontal force is applied to the tactile sensor's surface by an aluminum block, which is fixed to a six-axis force/torque sensor (Micro Mini, B.L. Autotech) and the triaxial stage. The six-axis force/torque sensor is used in order to monitor the applied force vector precisely. This reference force/torque sensor is calibrated so as to have a 0.06 N resolution in the -40 to 40 N range.

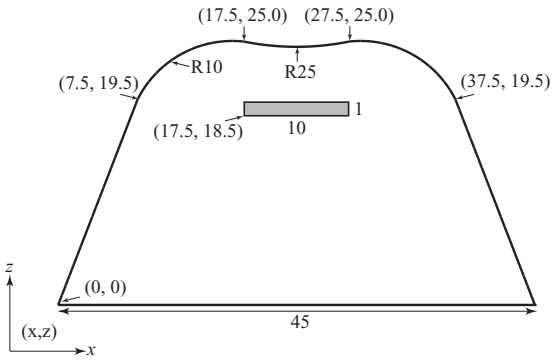

Fig. 5. Elastic layer

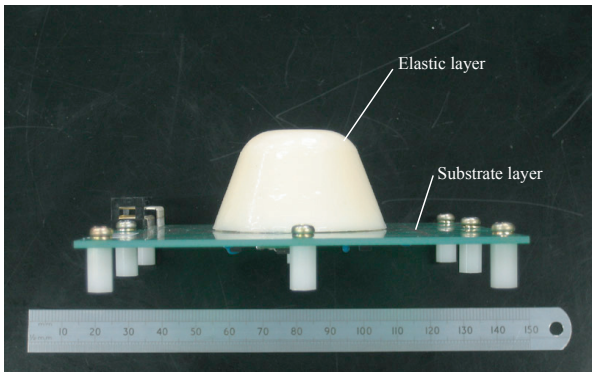

Fig. 6. Prototype of tactile sensor

The reference force sensor's outputs are sampled by a PC via a A/D converter board. The triaxial stage displaces the tactile sensor via the reference sensor and the aluminum block. The coordinate origin is at the center point of the elastic layer's surface. Before the following experiments, we set 77 reference points within $\pm$ directions of xy-axis and $-$ direction of z-axis.

Fig. 8 shows the calculation and measurement results of displacement of ± 2 mm xy-axis and of 2 mm z-axis. In the same way, Fig. 9 shows the results of displacement of ± 2 mm xy-axis and of 4 mm z-axis. The results of $y = -2$ mm in Fig. 9 have relatively large errors. One of these error's causes is an error accumulation. On the other hand, the other results have had small errors of roughly 5 percent, and the calculated results have been in good agreement with the applied displacements.

Fig. 10 and Fig. 11 shows the measured and the calculated force vectors. Because these force vectors are calculated from the displacement vectors, three points near $y = -1.5$ N in Fig. 11 has relatively large errors. Other calculated vectors are close to measured vectors. Though there have been a few variation, errors of the calculated vector have been roughly 10 percent.

C. Experiments of Slip

An acrylic block depressed the tactile sensor with a certain amount of force and slipped horizontally three times. Experimental settings are shown in Fig. 12, and this ex-

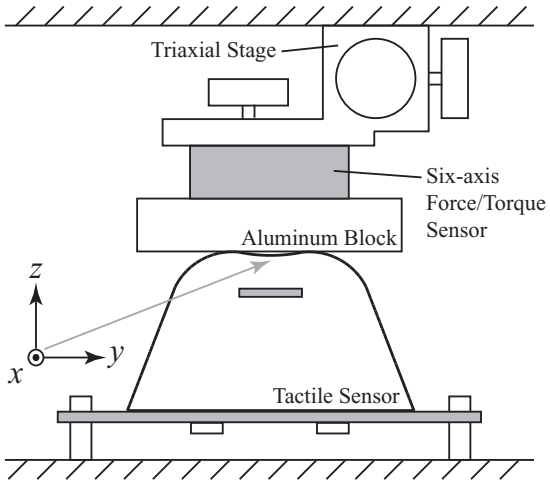

Fig. 7. Experimental setup of displacement and force vectors

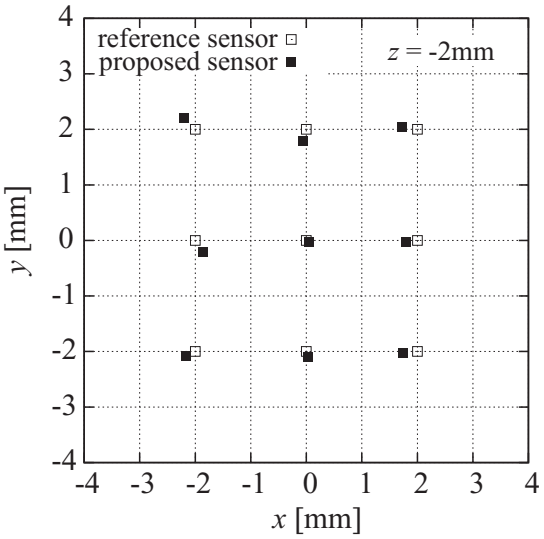

Fig. 8. Calculation vs, measurement displacement ($z = 2$ mm)

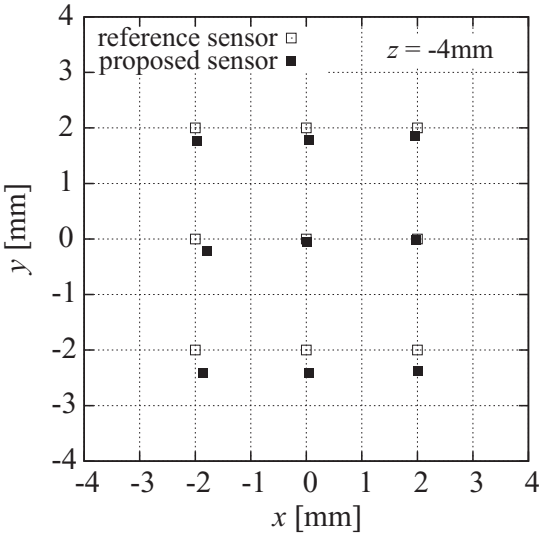

Fig. 9. Calculation vs, measurement displacement ($z = 4$ mm)

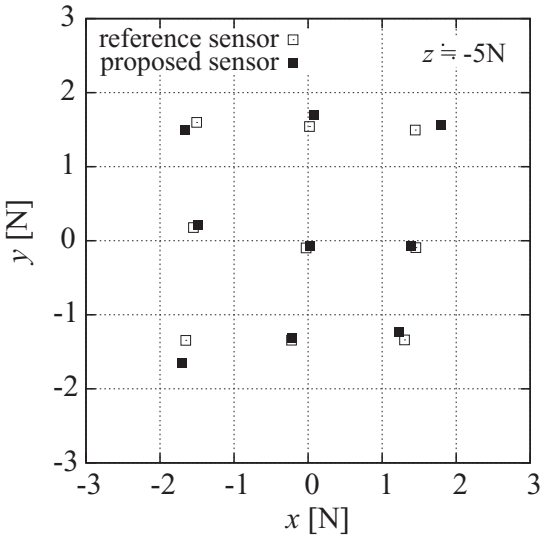

Fig. 10. Calculation vs, measurement force vectors at $z \simeq 5$ N

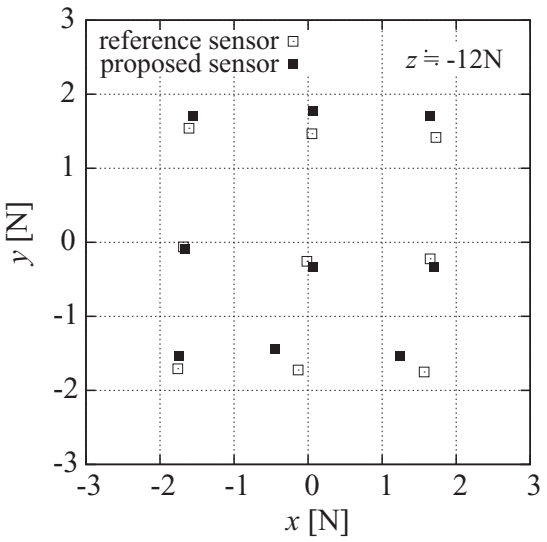

Fig. 11. Calculation vs, measurement force vectors at $z \simeq 12$ N

perimental result is shown in Fig. 13. The horizontal axis shows time steps of 1 ms. The left vertical axis shows the output voltages of the laser displacement meter and four inductors, and the right axis shows the slip detection. In this experiment, the output voltage of the laser displacement meter is corresponding to the share displacement of an elastic layer. In Fig. 13, there are three points in which the output voltage of the laser displacement meter increases rapidly after continous decline, and these indicate stick-slip phenomenon. The output voltages of the inductors become large at the three sliding moments. Therefore, the tactile sensor detected three slips by three sigma limits. Especially, in third stick-slip phenomena the change in output of the laser displacement meter is very slight (0.1 mm) and the change in output of four inductors are very small, but this sensor can detect slipping. In the result detail, there are some individual slip detections by the three sigma limits in each inductor. Moreover, the tactile sensor detected slips at only the three moments that all four inductors detected at the same moment. These results means that the proposed tactile sensor can detect slips precisely and has a robustness to partial slips. The detection rate was at 90 percent through repetitive experiments, and the tactile sensor was able to detect slips almost certainly.

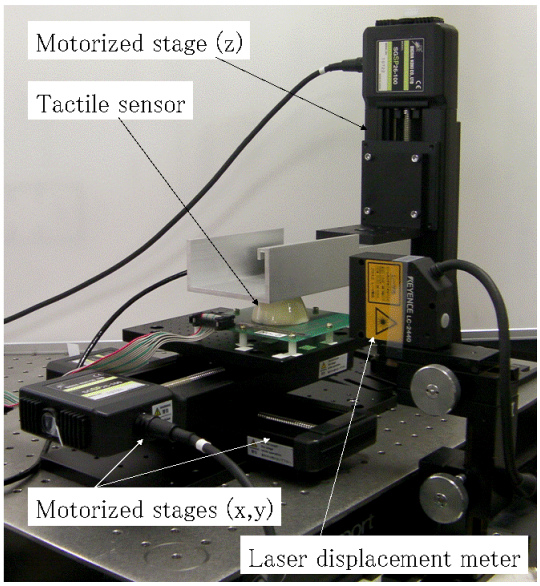

Fig. 12. Experimental setup of slip detection

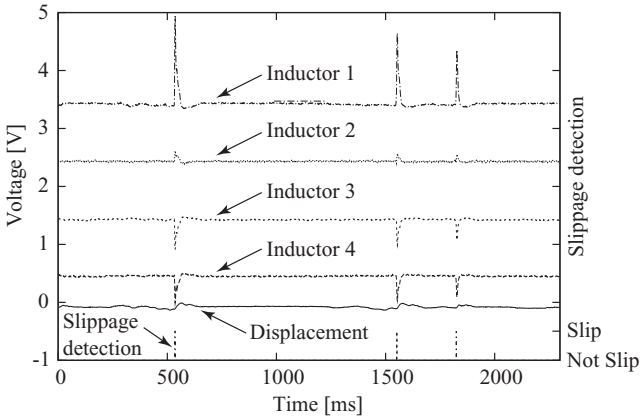

Fig. 13. Observed displacement and slip detection

We applied the tactile sensor to a two-fingered robot hand (Fig. 14). After the robot hand grasped an acrylic bar by 10 N, the acrylic bar was pulled down in the direction of an arrow in Fig. 14. The detection rate of the applied tactile sensor was at only 50 percent. One of causes of low rate was that the grasping force was too strong. It is necessary for the tactile sensor to be designed its softness and shape for a purpose.

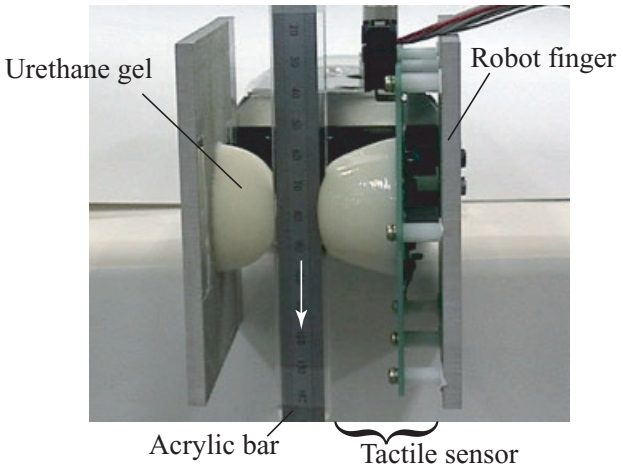

Fig. 14. Two-fingered robot hand with tactile sensor

IV. CONCLUSIONS AND FUTURE WORKS

A. Conclusions

In this paper, a magnetic type tactile sensor by GMR elements and inductors has been proposed. Features of the tactile sensor are a wiring reduction, simple structure and low cost. The tactile sensor provides two functions. First, the proposed sensor measures a force vector from GMR elements' output voltages. Second, the sensor detect a slip-stick phenomenon from inductors' output voltages. These two functions can work simultaneously and independently. The tactile sensor has calculated force vectors of roughly 10 percent and has detected slips robustly through laboratory experiments.

B. Future Works

The proposed tactile sensor can be created many variation in hardness and shape of the elastic layer. If the elastic layer is hard, the tactile sensor can measure a strong force, and vice versa. If the elastic layer is thick and soft, the tactile sensor becomes high sensitivity. Softness and shape of the elastic layer can be changed according to its purpose. Then, we establish a method to design elastic layers. Additionally, it is necessary to propose the system in which the influence of terrestrial magnetism is appropriately processed for expansion of sensor application.

Finally, our purpose is to realize a low cost and useful robot hand. We are going to downsize the tactile sensor in order to apply on fingertips of two- and multi-fingered robot hand.

REFERENCES

[1] Ch. Borst, M. Fischer, S. Haidacher, H. Liu and G. Hirzinger, "DLR Hand II: Experiments and Experiences with an Anthropomorphic Hand", *in Proc. IEEE Int. Conf. on Robotics and Automation*, 2003, pp.702-707.

[2] A. Namiki, Y. Imai, M. Ishikawa and Makoto Kaneko, "Development of a High-speed Multifingered Hand System and Its Application to Catching", *in Proc. IEEE/RSJ Int. Conf. on Intelligent Robots and Systems*, 2003, pp.2666-2671.

[3] W Fukui, H. Nakamoto, F. Kobayashi, F. Kojima, N. Imamura, T. Maeda, K. Sasabe, and H. Shirasawa, "Development of Multi-Fingered Universal Robot Hand", *Proc. of Joint 4th Int. Conf. on Soft Computing and Intelligent Systems and 9th Int. Symp. on Advanced Intelligent Systems*, 2008, pp.1117-1122.

[4] M.R. Tremblay and M.R. Cutkosky, "Estimating friction using incipient slip sensing during a manipulation task", *in Proc. IEEE Int. Conf. on Robotics and Automation*, vol.1, 1993, pp.429-434.

[5] BL AUTOTEC, LTD. FORCE TORQUE SENSOR, *https://www.bl-autotec.co.jp/english/index.html*.

[6] M. Kobayashi and S. Sagisawa, "Three direction sensing silicon tactile sensors", *IEICE Trans. Electron.*, vol.J74-C-II, no.5, 1991, pp.427-433.

[7] M. Ohka, I. Higashioka and Y. Mitsuya, "A micro optical three-axis tactile sensor (validation of sensing principle using model)," *Advances Information Storage Systems*, vol.10, 1999, pp.313-325.

[8] K. Nakamura and H. Shinoda, "" A tactile sensor instantaneously evaluating friction coefficients," in *Proc. 11th Int. Conf. on Solid - State Sensors and Actuators*, vol.2, 2001, pp.1430-1433.

[9] J.S. Son, E.A. Monteverde and R.D. Howe, "A tactile sensor for localizing transient events in manipulation," in *Proc. IEEE Int. Conf. on Robotics and Automation*, 1994, pp.471-476.

[10] J. Jockusch, J. Walter and H. Ritter, "A tactile sensor system for a three fingered robot manipulator," in *Proc. IEEE Int. Conf. on Robotics and Automation*, 1997, pp.3080-3086.

[11] S. Takenawa, "A Magnetic Type Tactile Sensor using a Two-Dimensional Array of Inductors", *Proc. IEEE Int. Conf. on Robotics and Automation*, 2009, pp.3295-3300.